

LINEAR INDUCTION MOTOR DESIGN AND APPLICATION

A Thesis

presented to

the Faculty of California Polytechnic State University,

San Luis Obispo

In Partial Fulfillment

of the Requirements for the Degree

Master of Science in Electrical Engineering

by

Yu-Shun Hsiao

June 2023

© 2023

Yu-Shun Hsiao

ALL RIGHTS RESERVED

## COMMITTEE MEMBERSHIP

**TITLE:** Linear Induction Motor Design and Application

**AUTHOR:** Yu-Shun Hsiao

**DATE SUBMITTED:** June 2023

**COMMITTEE CHAIR:** Majid Poshtan, Ph.D.  
Associate Professor  
Engineering Department

**COMMITTEE MEMBER:** Xiao-Hua(Helen) Yu, Ph.D.  
Professor  
Engineering Department

**COMMITTEE MEMBER:** Taufik, Ph.D.  
Professor, Director of Electric Power Institute  
Engineering Department

## ABSTRACT

Linear Induction Motor Design and Application

Yu-Shun Hsiao

This master's thesis explores the potential of Linear Induction Motors (LIMs) as a promising technology in the context of increasing eco-friendliness and electrical demand. The thesis begins with an overview of LIM, its unique characteristics, and fundamental principles. Experimental investigations are conducted on a laboratory-scale LIM with different coil connections, including parallel-delta, parallel-Y, series-delta, and series-Y. The impact of rail design, specifically T-shape rail and vertical rail, is also examined. Results show that the parallel-delta coil connection exhibits superior performance, while the use of T-shape rail enhances performance across different coil connections. Three future applications are proposed, accompanied by simple 3D models. This thesis contributes to understanding LIM technology, optimizing performance, and exploring potential applications.

**Keywords:** Linear Induction Motor, LIM, coil connections, rail design, performance optimization, future applications.

## ACKNOWLEDGMENTS

I want to express my deepest gratitude to my parents for their unwavering support and encouragement throughout my academic journey. Their love, understanding, and belief in my abilities have been invaluable.

I am sincerely grateful to Dr. Poshtan for his guidance, mentorship, and expertise throughout the entire process of this thesis. His insightful feedback, patience, and dedication have been instrumental in shaping and refining this research.

I would also like to extend my appreciation to the entire faculty and staff of Cal Poly for providing a conducive learning environment and access to resources that were essential for the successful completion of this thesis.

Furthermore, I would like to thank my friends and classmates for their camaraderie and for being a constant source of inspiration and motivation.

Lastly, I am grateful to all the participants and individuals who contributed their time and insights during the data collection phase of this research. Their willingness to participate and share their experiences has significantly enriched the findings of this thesis.

Without the support and contributions of all these individuals, this thesis would not have been possible. Thank you again for being a part of my academic journey and making this achievement a reality.

## TABLE OF CONTENTS

	Page
LIST OF TABLES .....	ix
LIST OF FIGURES .....	x
CHAPTER	
1 INTRODUCTION .....	1
1.1 Induction Motor .....	1
1.2 Rotational Induction Motor.....	1
1.3 Linear Induction Motor.....	2
1.4 Type of LIM .....	3
1.5 Linear Induction Application .....	4
2 BACKGROUND .....	6
3 THEORY .....	8
3.1 Fundamental of LIM .....	8
3.2 Slots and Winding Distribution.....	10
3.3 Slip in Linear Induction Motors.....	12
3.4 Magnetic Fields in Linear Induction Motors .....	14
3.5 Maxwell's equations .....	16
3.6 Faraday's Law in Linear Induction Motors .....	17
3.6.1 Eddy Currents .....	19
3.7 Lenz's Law in Linear Induction Motors .....	20
3.8 Power Factor .....	21
3.9 End Effect .....	23
3.10 Efficiency of the motor .....	24
4 ANALYSIS .....	26
4.1 Linear Induction Motor Modeling .....	26
4.2 Data Collection Setup .....	27

4.3 Rails selection .....	29
4.4 Coils Connection.....	29
4.4.1 Parallel-Delta connection.....	30
4.4.2 Parallel-Y Connection.....	31
4.4.3 Series-Delta Connection .....	32
4.4.4 Series-Y Connection .....	33
5 TESTING RESULT .....	35
5.1 Parallel-Delta connection.....	35
5.1.1 Vertical Rail .....	35
5.1.2 T-Shape Rail.....	36
5.2 Parallel-Y Connection.....	37
5.2.1 Vertical Rail .....	37
5.2.2 T-Shape Rail.....	38
5.3 Series-Delta Connection .....	39
5.3.1 Vertical Rail .....	39
5.3.2 T-Shape Rail.....	41
5.4 Series-Y Connection .....	41
5.4.1 Vertical Rail .....	42
5.4.2 T-Shape Rail.....	43
5.5 Result Analysis.....	44
6 LIM APPLICATION .....	47
6.1 Snowmobile .....	47
6.2 E-Bike .....	48
6.3 Elevator .....	49
7 FUTURE WORK.....	52
7.1 Size and Geometry.....	52
7.2 Material Selection .....	52
7.3 Coil Connection Design.....	52

7.4 Rail Selection .....	53
7.5 Power Electronics .....	53
7.6 Testing .....	53
7.7 Safety .....	54
8 CONCLUSION .....	55
BIBLIOGRAPHY .....	57

## LIST OF TABLES

Table	Page
5.1 Parallel-Delta with Vertical Rail-120V Input data collection .....	36
5.2 Parallel-Delta with T-Shape Rail-120V Input data collection .....	37
5.3 Parallel-Y with Vertical Rail 120V Input data collection .....	38
5.4 Parallel-Y with T-shape Rail 120V Input data collection .....	39
5.5 Series-Delta with Vertical Rail 120V Input data collection .....	40
5.6 Series-Delta with T-Shape Rail-120V Input data collection .....	41
5.7 Series-Y with Vertical Rail 120V Input data collection .....	42
5.8 Series-Y with T-Shape Rail 120V Input data collection .....	43
5.9 Force Comparison .....	44

## LIST OF FIGURES

1.1	Induction Motor .....	2
1.2	Linear Induction Motor .....	2
1.3	Singe-sided Linear Induction Motor .....	3
1.4	Double-Sided Linear Induction Motor .....	4
2.1	Rotation Motor v.s Linear Motor .....	7
3.1	LIM Slot Plot .....	11
3.2	Slip v.s. Velocity .....	13
3.3	LIM Slip concept .....	14
3.4	FEMM LIM simulation Example .....	15
3.5	Eddy Current .....	20
3.6	Power Factor .....	22
4.1	LIM SolidWorks Modeling .....	27
4.2	Physical Setup of the Testing .....	28
4.3	Example: Parallel Delta connection .....	28
4.4	T-Shape Rail vs Vertical Rail .....	29
4.5	LIM Coils .....	30
4.6	Parallel-Delta connection .....	31
4.7	Parallel-Y Connection .....	32
4.8	Series-Delta Connection .....	33
4.9	Series-Y Connection .....	34
5.1	Parallel-Delta with Vertical Rail-120V Input .....	36

5.2	Parallel-Y with Vertical Rail 120V Input .....	38
5.3	Series-Delta with Vertical Rail 120V Input .....	40
5.4	Series-Y with Vertical Rail 120V Input .....	42
5.5	Pulling force comparison .....	44
5.6	Force Improvement due to T-Shape Rail .....	45
6.1	LIM Snowmobile SolidWork .....	47
6.2	LIM Snowmobile Design .....	48
6.3	LIM E-Bike Application .....	49
6.4	LIM elevator Application .....	50
6.5	LIM elevator Application 2nd .....	51
6.6	LIM elevator SolidWork .....	51

# **Chapter 1**

## **INTRODUCTION**

### **1.1 Induction Motor**

An induction motor is a type of AC motor that uses electromagnetic induction to produce rotational force. It consists of a stator, which houses the stationary windings, and a rotor, which is a rotating part of the motor. When an AC voltage is applied to the stator windings, a rotating magnetic field is produced which induces currents in the rotor. The interaction between the magnetic fields produces torque, causing the rotor to rotate[1].

### **1.2 Rotational Induction Motor**

Rotational Induction Motors are widely used in many industrial, commercial, and residential applications. They are used in HVAC systems, refrigerators, washing machines, pumps, compressors, and other machines that require continuous speed control. Rotational Induction Motors are preferred over other types of motors because of their simple and rugged construction, low cost, high reliability, and ease of maintenance[2].

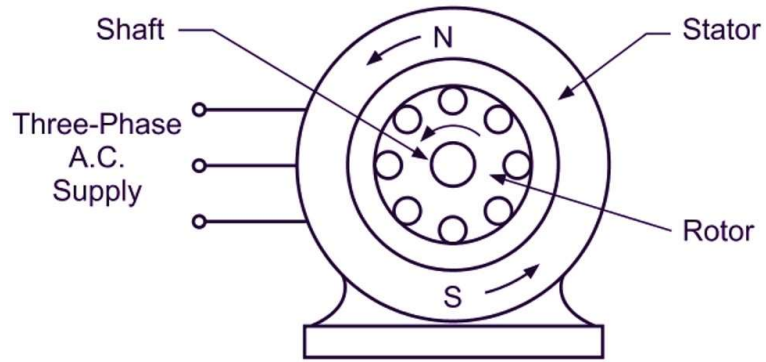


**Figure 1.1: Induction Motor**

### 1.3 Linear Induction Motor

A linear induction motor (LIM) is a type of motor that produces force in a straight line instead of rotational force. The working principle of a LIM is similar to that of a rotational induction motor. However, in a LIM, the rotor is replaced with a translator or mover that moves along a track. When an AC voltage is applied to the stator windings, a magnetic field is produced that interacts with the magnetic field of the translator, producing force and causing it to move along the track.

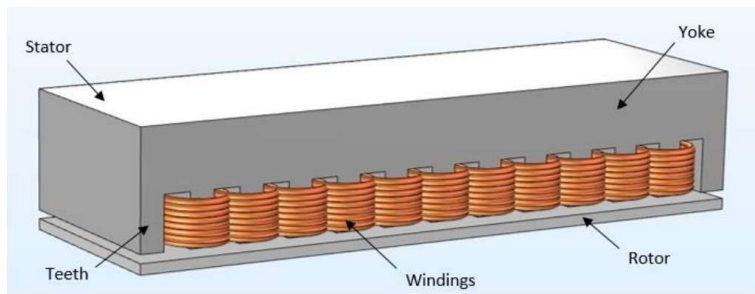


**Figure 1.2: Linear Induction Motor**

## 1.4 Type of LIM

Linear induction motors (LIMs) can be categorized into different types based on the number of primary and secondary windings used in the motor construction. In general, there are two types of LIMs that are commonly used: single-sided and double-sided LIMs.

A single-sided LIM, also known as a single-sided linear induction motor (SLIM), consists of a primary winding and a secondary reaction plate. The primary winding is usually placed above the secondary reaction plate, and the secondary plate is free to move along a track or rail system. When the primary winding is energized with a three-phase AC supply, a magnetic field is generated, which interacts with the secondary reaction plate, causing it to move.

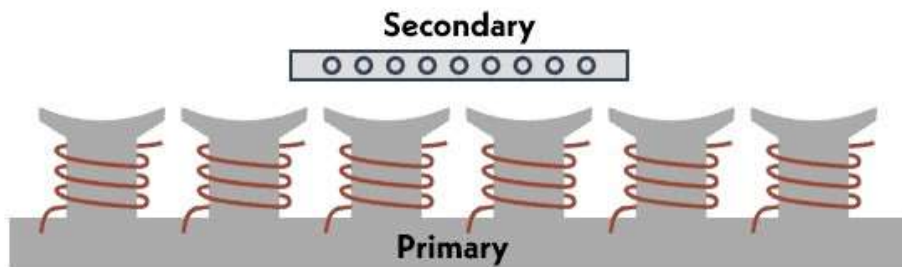


**Figure 1.3: Singe-sided Linear Induction Motor**

On the other hand, a double-sided LIM, also known as a double-sided linear induction motor (DLIM), consists of two primary windings and one secondary reaction plate. The primary windings are placed on either side of the secondary reaction plate, and the secondary plate is free to move between them. When the primary windings are energized with a three-phase AC supply, a magnetic field is generated, which interacts with the secondary reaction plate, causing it to move.

Both SLIMs and DLIMs have their own advantages and disadvantages, and the

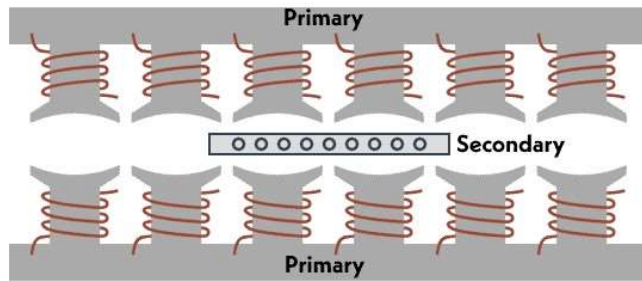


**Figure 1.4: Double-Sided Linear Induction Motor**

choice between the two types depends on the specific application requirements. Single-sided LIMs are simpler in construction and can be used for applications where a smaller force is required. Double-sided LIMs, on the other hand, can generate higher forces and are more suited for heavy-duty applications. However, they are more complex in construction and require more power to operate.

In this thesis, we focused on a double-sided LIM with two primary and one secondary winding.

## 1.5 Linear Induction Application

Linear Induction Motors (LIMs) have a unique ability to produce linear motion without the use of gears or other mechanical components, making them ideal for applications where high speed and precision are required. One of the most well-known applications of LIMs is in the transportation industry, where they are used in high-speed trains such as maglev trains, which can travel at speeds of over 500 km/h.

LIMs are also used in material handling systems, such as conveyor belts and escalators, where they provide precise and efficient movement of materials and people.

In addition, LIMs are used in many scientific and research applications, such as linear accelerators and particle accelerators, where high precision and accuracy are

required.[4]

# **Chapter 2**

## **BACKGROUND**

Induction motors have been widely used in various industrial, commercial, and residential applications for over a century due to their simple and rugged construction, low cost, high reliability, and ease of maintenance. The development of induction motors has significantly contributed to the growth of many industries by providing efficient and reliable energy conversion. Induction motors can be classified into two types: rotational induction motors and linear induction motors.

Rotational induction motors are the most commonly used type of induction motors, and they are used in a wide range of applications, from small appliances to large industrial machinery. The principle of operation of a rotational induction motor is based on the interaction between the stator and rotor magnetic fields, which produce torque and rotational motion.

Linear induction motors, on the other hand, produce linear motion without the use of mechanical components such as gears or cams. Linear induction motors are used in various applications such as maglev trains, conveyor systems, and material handling systems. They have advantages over conventional mechanical systems due to their high efficiency, precise control, and low maintenance requirements.

Picture 2.1 shows a comparison between a rotational induction motor and a linear induction motor. The image highlights the main difference between the two types of motors: while the rotational induction motor produces rotational motion, the linear induction motor produces linear motion. Both types of motors use the principle of electromagnetic induction

to convert electrical energy into mechanical energy, but they are designed for different applications.

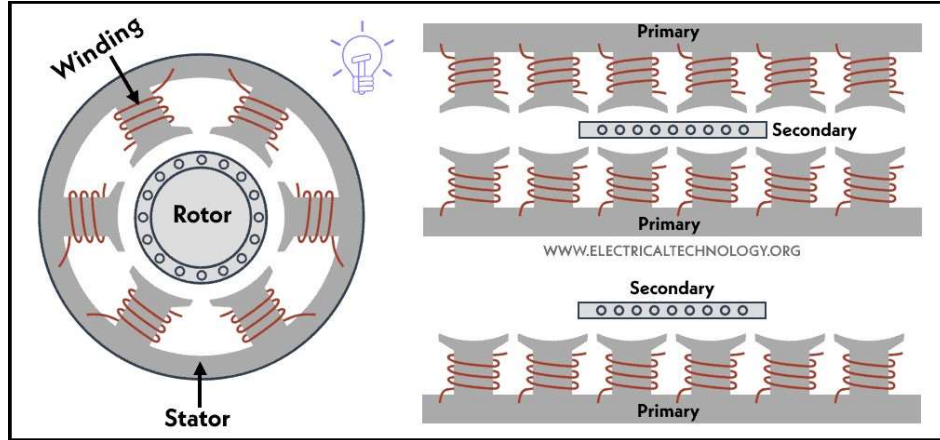


**Figure 2.1: Rotation Motor v.s Linear Motor[7]**

The use of induction motors has become increasingly important in recent years due to the growing demand for energy-efficient and eco-friendly technologies. Therefore, research and development in this field have been ongoing to improve the performance and efficiency of induction motors.

This master thesis aims to investigate and analyze the performance of linear induction motors. The study will include a detailed analysis of the operating principles, design, and applications of these motors. The research will also focus on the efficiency and performance of these motors, with an emphasis on identifying the factors that affect their efficiency and performance. The findings of this study will provide valuable insights for the improvement of these motors and their applications in various fields.

# **Chapter 3**

## **THEORY**

### **3.1     Fundamental of LIM**

A linear motor operates on similar principles as a rotary motor, but with the notable distinction that it generates motion in a linear direction rather than rotational. The key to achieving this linear motion is the induction of a traveling stator field through polyphase excitation. This process involves exciting the stator windings with multiple phases of alternating current, which generates a magnetic field that travels along the length of the motor.

To visualize the construction of a linear motor, one can imagine slicing a rotary motor down its center and unrolling the split stator and rotor. The resulting linear motor consists of elongated stator and rotor components, aligned in a linear configuration. All the essential parts of the rotary motor, such as the windings, are still present in the linear motor, but their shape conforms to the linear arrangement.

One significant difference between the linear motor and its rotary counterpart is the presence of open-ended air gaps at each end of the linear motor. These air gaps, which are absent in the rotary motor, give rise to what is known as "end-effects." These end-effects introduce unwanted losses and reduce the performance of the linear motor. Understanding and mitigating these end-effects is a specialized topic in itself, which is beyond the scope of this discussion. However, it is important to acknowledge their impact on the overall performance of the linear motor.

Another distinction between the linear and rotary motors lies in the design of the rotor. In a rotary motor, conductive bars or end rings are used to facilitate the flow of eddy currents, creating a low-impedance circuit. However, in the linear motor, a simplified conductive plate or blade is employed as the rotor. This solid conductive plate allows the traveling stator field to distribute continuously along its surface, as dictated by Maxwell's Equations. Unlike the rotary case, the field cannot be influenced or controlled as easily. This difference in rotor design reflects a trade-off between manufacturing simplicity and optimal performance.

One efficiency consideration is the comparison between the "Squirrel Cage Rotor" used in the rotary motor and the "Blade Rotor" used in the linear motor. At higher speeds, the sheet rotor of the linear motor is only marginally less efficient than the squirrel cage rotor, with a difference of around 5-10%. Attempts to recover this efficiency loss in the linear motor have involved incorporating optimized holes in the rotor blade to create a path for induced eddy currents to flow. However, such measures significantly increase the complexity of design and manufacturing without providing noticeable performance improvements.

In addition to the aforementioned differences, the linear motor offers greater flexibility in terms of which part of the motor can be fixed and which part can move, depending on the specific application. For example, in a Pod or Hyperloop vehicle, the stator can be fixed onboard the moving Pod, while the rotor blade is fixed to the track. In this scenario, the rotor becomes the fixed part, and the stator is technically considered to be in motion. This flexibility in motor configuration allows for various design options based on specific requirements.

Linear motors can be classified into different types or configurations, with the main categorization being synchronous and asynchronous motors. Asynchronous motors, also known as induction motors, utilize the principle of induction to generate the attractive

Lorentz force required for motion. In this thesis, a linear induction motor (LIM) is chosen as the motor type, primarily due to its simpler design compared to synchronous motors. Synchronous motors involve the use of permanent magnets to create the required force, making them more complex in design.

While the focus of this thesis is on linear induction motors, it is worth noting that other types of linear motors exist, offering a range of choices and options for various linear motor configurations.

## 3.2 Slots and Winding Distribution

The traveling stator field in a linear motor is ideally a sine wave produced by the sum of the three-phase delayed currents. However, achieving a perfect sine wave is expensive and impractical. Therefore, in practice, the sine wave stator field is approximated by square waves. To improve this approximation, the number of slots in the stator core is increased[5].

By increasing the number of slots, the windings have more opportunities to interact and "smooth" the stator field, making it more sine-like and gradual. This improvement can be observed both in the time domain and frequency domain. A sine-like stator field helps in the frequency domain by reducing the higher-order harmonics that can disrupt the fundamental frequency, which represents the thrust force moving the motor. These higher harmonics act as a braking force and can lead the motor towards other synchronous speeds, decreasing its performance.

The technique of using distributed windings, where the windings are spread across multiple slots, helps achieve a better approximation of the sine wave stator field. Increasing the number of slots in the stator core leads to a more sine-like approximation. However, there is a point of diminishing returns, where adding more slots no longer significantly improves the sine wave distribution and starts resembling a triangle waveform. To address

this, a single slot winding for each phase can be shifted to the left or right. This shifting helps round out the peaks of the sine wave, improving its approximation.

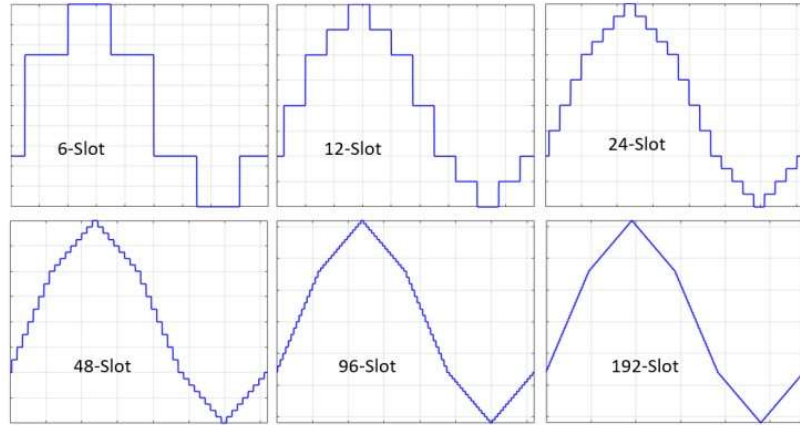


**Figure 3.1: LIM Slot Plot**

Figure 3.1 gives a better idea of what happened if we increase the slot of the motor. We can also see that after 96- Slot, there is not much of a change to the sine wave.

While this shifting technique is commonly used in rotary motors, implementing it in linear motors is challenging due to the complexity of winding the coils and maintaining balance. Bringing the last coil to the front of the motor for the shifted configuration requires intricate winding schemes and results in an unbalanced system.

However, this shifting scheme does improve the approximation of the stator sine wave by smoothing out the peaks.

In summary, increasing the number of slots in the stator core improves the approximation of the sine wave distribution in the stator magnetic traveling field. This leads to a reduction in other harmonics, enhancing the motor's efficiency and driving thrust. The slots and windings are crucial elements in the design of a linear induction motor, contributing to its performance and behavior.

### 3.3 Slip in Linear Induction Motors

In a linear asynchronous motor, the stator field created by the 3-phase excitation has a velocity known as the synchronous speed ( $V_s$ ). This speed is directly related to the frequency of the stator field ( $f_s$ ). As the stator field sweeps across the rotor, it induces an equal and opposite magnetic field in the rotor. This opposing rotor field creates a repulsive force between the rotor and the stator, resulting in the primary linear movement of the motor, known as thrust.

However, it's important to note that the rotor also develops its own traveling magnetic field with its own speed ( $V_r$ ) and frequency ( $f_r$ ). The rotor field is slightly slower compared to the stator field, which creates a "delay" or slip between the two fields. The slip of an asynchronous motor is defined as the difference between the synchronous speed of the stator field and the actual mechanical speed of the rotor. Mathematically, it is expressed as:

$$S = \frac{V_s - V_r}{V_s} \quad (3.1)$$

The slip value ranges between 0 and 1, where a slip of 1 corresponds to no movement (rotor stationary relative to the stator field), and a slip of 0 means the rotor has reached the synchronous speed. A plot of slip against the rotor velocity helps visualize its characteristics during motor operation.

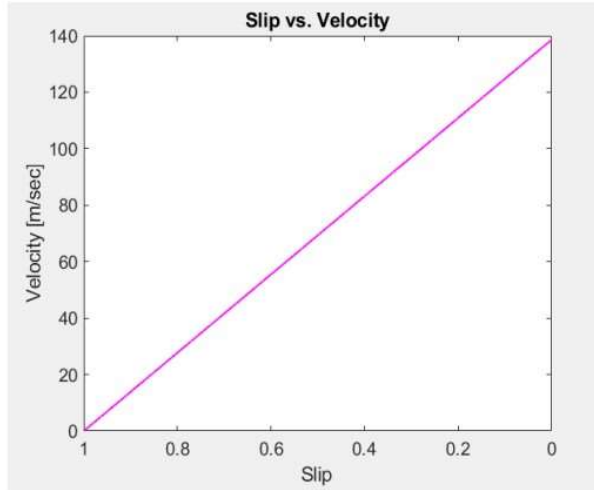


**Figure 3.2: Slip v.s. Velocity[6]**

At full slip (slip = 1), the rotor velocity is 0 m/sec, and at slip = 0, the rotor reaches the synchronous speed of the stator field (138.89 m/sec or 500 km/h). When slip is 1, there is the largest difference between the stator field velocity and the actual velocity of the rotor. As slip approaches 0, the rotor's velocity approaches the synchronous speed, and there is minimal difference between the two velocities.

It's important to note that the rotor cannot move faster than the synchronous speed of the stator field. Once the synchronous speed is reached, the rotor stops accelerating. This concept can be visualized with the help of 3.3, which displays a 2-slot stator above a blade rotor in two scenarios: 1) when slip equals 1 (stationary motor) and 2) when slip equals 0 (motor moving at synchronous speed).

As the motor approaches synchronous speed, less force is generated, but the velocity increases. It's worth exploring the thrust curve in the Lorentz Force section

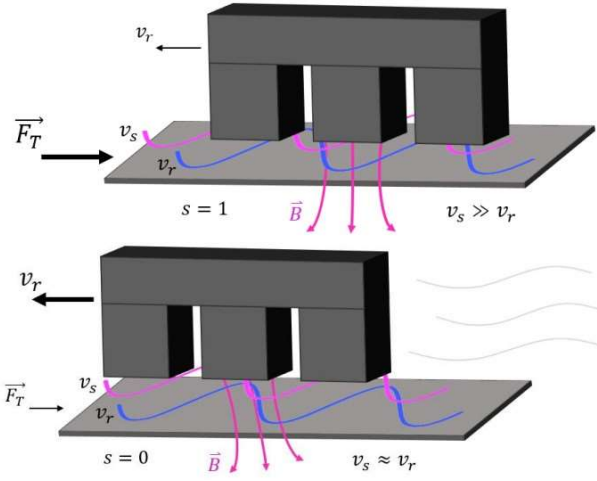


**Figure 3.3: LIM Slip concept[6]**

to gain a deeper understanding. At the synchronous speed, no additional thrust is generated by the motor.

### 3.4 Magnetic Fields in Linear Induction Motors

Magnetic fields play a critical role in the operation of linear induction motors (LIMs). LIMs use electromagnetic induction to produce a force that drives the motor. This force is generated by the interaction between the magnetic field produced by the stator winding and the conductive rotor. Figure 3.4 shows a cross-section view of a "Magnetic River" which is a LIM, simulated using the Finite Element Method Magnetics (FEMM) software. The image is colored to indicate the distribution of electric current density within the motor, with different colors representing different intensities of current flow. The overall shape of the motor appears to be a long, rectangular channel with a series of coils positioned along its length.

In a LIM, the stator winding produces a varying magnetic field, which interacts

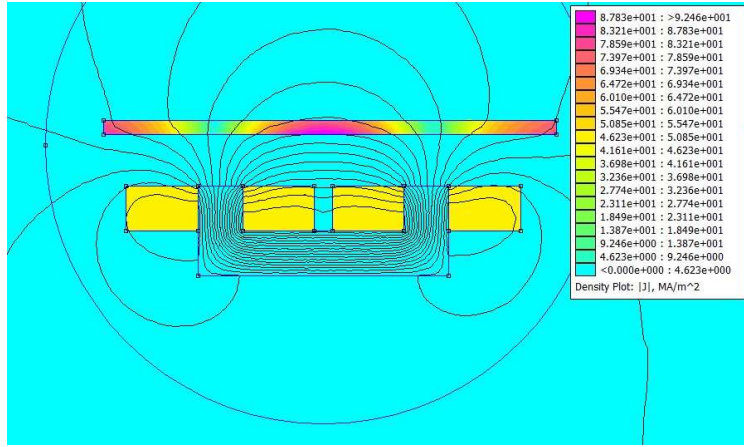


**Figure 3.4: FEMM LIM simulation Example[6]**

with the rotor to induce an electromotive force (EMF) and generate a current in the rotor. This current, in turn, generates a magnetic field that interacts with the stator magnetic field to produce a force that drives the rotor.

The strength and direction of the magnetic field in a LIM depend on various factors, such as the geometry of the motor, the current in the stator winding, and the materials used in the construction of the motor. The magnetic field can be visualized using magnetic field lines, which represent the direction and strength of the magnetic field at each point in space.

The magnetic field in a LIM can be calculated using Maxwell's equations, which describe the behavior of electric and magnetic fields. These equations are used to determine the magnetic flux density, which is a measure of the strength of the magnetic field. The magnetic flux density is proportional to the current in the stator winding and inversely proportional to the distance between the stator and rotor.

Optimizing the magnetic field in a LIM is essential for maximizing the force generated by the motor and improving its efficiency. By adjusting the geometry of the motor and the current in the stator winding, motor designers can optimize the magnetic field to produce the desired force and minimize energy losses due to Lenz's law.

## 3.5 Maxwell's equations

Maxwell's Equations are a set of fundamental equations that govern electromagnetics. They describe the relationships between electric and magnetic fields, currents, and charges. These equations are essential for understanding the principles of the linear induction motor (LIM) and its operation.[4]

In their differential form, the equations are as follows:

$$\nabla \times \vec{B} = -\frac{\partial \vec{B}}{\partial t} \quad (3.2)$$

This equation, derived from Faraday's Law, states that a changing magnetic field induces an electric field.

$$\nabla \times \vec{H} = \vec{J} + \frac{\partial \vec{D}}{\partial t} \quad (3.3)$$

Ampere's Law is represented by this equation. It states that a changing electric field produces a magnetic field and that currents can also generate magnetic fields.

$$\nabla \times \vec{D} = \rho_v \quad (3.4)$$

Derived from Gauss's Law, this equation relates the electric flux density ( $B$ ) to the local charge density ( $\rho_v$ ).

$$\nabla \times \vec{B} = 0 \quad (3.5)$$

This equation, also derived from Gauss's Law, states that magnetic field lines form closed loops and do not have magnetic monopoles.

These equations highlight the interplay between electric and magnetic fields, currents, and charges. They are complemented by material relations expressed in equations 3.10 to 3.13:

$$\vec{D} = \epsilon \vec{E} \quad (3.6)$$

Electric flux density ( $D$ ) is related to electric field strength ( $E$ ) through the absolute permittivity ( $\epsilon$ ).

$$\vec{B} = \mu \vec{H} \quad (3.7)$$

Magnetic flux density ( $B$ ) is related to magnetic field strength ( $H$ ) through the absolute permeability ( $\mu$ ).

$$\vec{J} = \sigma \vec{E} \quad (3.8)$$

The electric current density ( $J$ ) is determined by the electric field strength ( $E$ ) and the conductivity ( $\sigma$ ).

These relations incorporate the properties of the medium through relative permittivity ( $\epsilon_r$ ) and permeability ( $\mu_r$ ) as well as the permittivity ( $\epsilon_0$ ) and permeability ( $\mu_0$ ) of free space or vacuum.

## 3.6 Faraday's Law in Linear Induction Motors

The traveling stator field in a linear motor is generated by exciting the stator windings with a three-phase source, where each input is out of phase with the others by 120 degrees. When the windings are excited, an electric potential develops across each coil winding, causing a current to flow through them. This changing electric potential across the coil

windings gives rise to a magnetic field and flux around the coil. This phenomenon is explained by Faraday's Law, which states that a change in flux induces an electromotive force (EMF) or voltage across the coil windings[7].

Equation 3.9 shows the equation of Faraday's Law. Where  $\epsilon$  is the electromotive force or EMF (proportional to an induced voltage drop across a coil),  $N$  is the turn number of that coil, and  $\phi_B$  is the flux around this coil. There is a negative sign in the equation because of Lenz's Law and will be discussed in the section below.

$$\epsilon = -N \frac{d\phi_B}{dt} \quad (3.9)$$

The stator windings can be modeled as inductors that store energy in a magnetic field when current passes through them. Changes in the electric potential at the ends of the coil affect the amount of current flowing through the windings, resulting in a proportional change in the magnetic field as the inductor resists the change in current. Similarly, if the magnetic field changes over time, the field collapses around the inductor and induces a current in the coil windings. This is the principle of electromagnetic induction, described by Faraday's Law[7].

In the linear motor, induction occurs due to the electric potential dropped across the stator windings. This induces a proportional current flow, generating the stator magnetic field according to Faraday's Law. The stator magnetic field varies in position and sweeps across the length of the stator due to the simultaneous excitation from the three-phase source[8].

As the traveling stator magnetic field sweeps across the stator, it interacts with the rotor and induces eddy currents according to the Maxwell-Faraday Law. The time-varying magnetic field from the stator creates an electric field strength, which is analogous to an electric current. These induced eddy currents in the conductive rotor, known as eddy

currents, contribute to thrust generation in the linear induction motor. This induction phenomenon forms the basis of the working principle of an asynchronous motor, as reflected in the name "linear induction motor."<sup>[8]</sup>

$$\nabla \cdot \vec{E} = -\frac{\partial \vec{B}}{\partial t} \quad (3.10)$$

### 3.6.1 Eddy Currents

The generation of eddy currents in the rotor is a result of the electromotive force (EMF) across a particular stator winding. Once induced in the rotor by the traveling stator field, these eddy currents create an equal and opposite magnetic field of their own. This process follows the same principles by which the eddy currents themselves were produced, but in reverse order. While the induced currents were initially generated by a time-varying magnetic field, the time-varying eddy currents now generate a magnetic field. This resulting magnetic field is equal and opposite to the original stator field from the source.

As a result, equations 3.9 and 3.10 sustain each other, similar to the behavior of a propagating electromagnetic wave. Furthermore, just like the stator field is produced from three-phase alternating currents, the newly created field from the eddy currents is also three-phase and alternating. These characteristics allow the rotor field to sweep across the length of the motor, similar to the traveling stator field. The interaction between the traveling stator field and the induced eddy currents in the rotor, along with the subsequent production of the corresponding magnetic field, is illustrated in Figure 3.5.

In Figure 3.5, the traveling stator field (pink) sweeps past the rotor, inducing eddy currents (light blue) that, in turn, generate an equal and opposite magnetic field in the rotor (dark blue). These fields are self-sustaining as long as the source is present.

The force (black) shown in Figure 3.5 acts on the plate to propel the motor<sup>[4]</sup>.

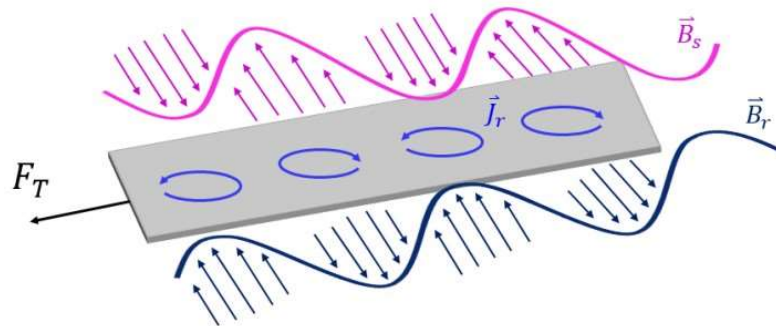


**Figure 3.5: Eddy Current**

### 3.7 Lenz's Law in Linear Induction Motors

Lenz's law is a consequence of Faraday's law of electromagnetic induction, which states that an induced electromotive force (EMF) generates a current that creates a magnetic field that opposes the change in magnetic flux that produced the EMF. Lenz's law applies to linear induction motors (LIMs), which use electromagnetic induction to produce a force that drives the motor.

In a LIM, the alternating current (AC) applied to the stator winding produces a varying magnetic field that interacts with the conductive rotor to induce an EMF.

The EMF generates a current in the rotor, which produces a magnetic field that opposes the change in magnetic flux that produced the EMF. This is Lenz's law in action.

Lenz's law is important in LIMs because it explains the direction of the induced current in the rotor. The induced current produces a magnetic field that interacts with the stator magnetic field to generate a force that drives the rotor. The direction of the induced current is opposite to the direction of the stator magnetic field, which is necessary to generate a force that moves the rotor.

Lenz's law is also important in understanding the efficiency of LIMs. The opposing magnetic field generated by the induced current in the rotor requires energy to produce, which results in a loss of efficiency. By optimizing the design of the LIM, motor designers can minimize the energy loss due to Lenz's law and improve the efficiency of the motor.

The Lorentz force equation describes the force experienced by a charged particle in an electric and magnetic field. In the case of a LIM, the force produced on the rotor can be expressed by the equation:

$$F = Q(E + v \times B) \quad (3.11)$$

where F is the force, q is the charge on the rotor, E is the electric field, v is the velocity of the rotor, and B is the magnetic field.

### 3.8 Power Factor

In the Polyphase Excitation section, we discussed the 3-phase system in terms of the three currents, each offset from one other by  $120^\circ$ . However, this configuration can also be described in terms of voltage. Similar to Figure 3.6, a phase diagram can depict both the voltages and currents with angular separation between them.[4]

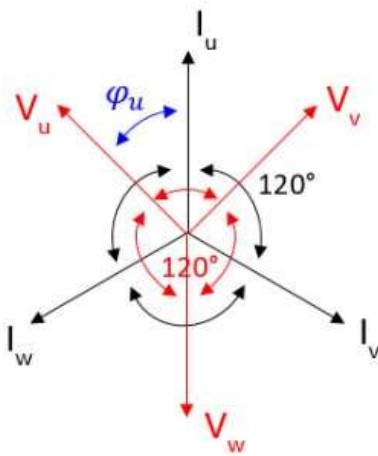


**Figure 3.6: Power Factor[4]**

Asynchronous motors typically have a power factor of around 0.8. A higher power factor indicates greater efficiency. In Equation 3.12, a power factor of one corresponds to a smaller angular separation between the voltages and currents, meaning they are in phase. This condition implies that all the energy supplied by the source is consumed by the load.

$$\text{Power Factor} = \frac{\text{Active Power}}{\text{Apparent Power}} = \cos(\psi) \quad (3.12)$$

In a purely inductive coil, a phase shift of  $90^\circ$  results in a power factor of zero. In this state, all the power in the system is reactive power, with no real power being dissipated. The inductor absorbs power on the positive swing and returns it to the system on the negative swing, avoiding power loss. However, in motor windings, the phase angle is not perfectly  $90^\circ$ , so there will always be some power dissipation due to losses in converting electrical energy to mechanical energy.

The windings in the motor are not purely inductive anymore because there are resistive losses present. As a result, the power factor is a positive value between zero and one. The

inductor windings feed energy back into the system during the downswing and absorb energy during the upswing, but some energy is lost in the process.

The voltage drop across an inductor is highest when the instantaneous current changes most rapidly, typically when it crosses the zero line. This leads to the voltage "leading" the current or, conversely, the current "lagging" behind the voltage.

$$\text{Power Factor} = \cos(\tan^{-1}\left(\frac{\pi \times p_s \times g}{\mu_0 \times s \times \tau_p \times v_s}\right)) \quad (3.13)$$

The power factor for a linear motor is defined by equation 3.13, which depends on the motor's design parameters such as secondary resistivity ( $p_s$ ), air gap distance (g), slip (s), synchronous speed ( $v_s$ ), and pole pitch ( $\tau_p$ ). It is known that  $\tau_p v_s$  is typically large in high-speed motors, allowing for a larger air gap without significantly affecting the power factor[6]. This property is important because the air gap distance plays a role in defining the motor's thrust and reducing it can be challenging, as explained in the Motor Design section.

### 3.9 End Effect

End-effects in a linear motor refer to decreases or losses in performance caused by the open-ended air gaps at the motor's ends. These air gaps differentiate linear motors from rotary motors and have a significant impact on thrust, power factor, and efficiency, all of which are reduced due to end-effects. Unlike rotary machines, which are continuous and circular, linear motors have distinct "beginning" and "end" points, causing an interruption in the field.

At low speeds, end-effects are not significant, but they become problematic at higher speeds. The magnetic field distribution in the air gap varies at the ends compared to the middle of the motor due to differences in wave velocity of the entering and exiting stator fields. The slow decay rate of these fields allows them to interfere with the main stator field's phase distribution, degrading performance[6].

One approach to mitigate end-effects is to operate the motor in a low-slip region near the synchronous speed. By using a variable speed or frequency drive, the motor can be kept in this region, where end-effects are minimized. Adjusting parameters such as air gap distance, pole number, supply frequency, and secondary resistivity can also help reduce end-effects, although it may involve a trade-off in motor performance.

Winding configuration adjustments can also mitigate end-effects. Proper techniques, like increasing the number of slots or windings per phase, ensure a symmetric and gradual phase distribution throughout the motor, approximating a smoother travelling stator field. This reduces the disruption caused by end-effects and makes the field distribution in the air gap appear less discontinuous to the secondary.

Another technique involves making the end teeth larger, capturing more of the field and increasing overall thrust. This compensates for the slight saturation observed in simulations at the end teeth, improving motor performance.

### **3.10 Efficiency of the motor**

The efficiency of the LIM can be expressed by the equation:

$$\eta = \frac{P_{out}}{P_{in}} \quad (3.14)$$

where  $\eta$  is the efficiency,  $P_{\text{out}}$  is the output power of the motor, and  $P_{\text{in}}$  is the input power of the motor.

# **Chapter 4**

## **ANALYSIS**

### **4.1 Linear Induction Motor Modeling**

In order to better understand the LIM being tested, a 3D model was created using SolidWorks. The purpose of the model was to show the details of the LIM and aid in the design and analysis process.

SolidWorks is a popular computer-aided design (CAD) software used in many engineering fields. Its features, including the ability to create complex 3D models and perform simulations, make it a powerful tool for designing and testing machines like the LIM.

The 3D model created using SolidWorks includes the idea of the various components of the LIM, including the stator and the rotor. The model shows the shape and size of each component, as well as their orientation and relationship to one another. Figure 4.1 shows the LIM model.

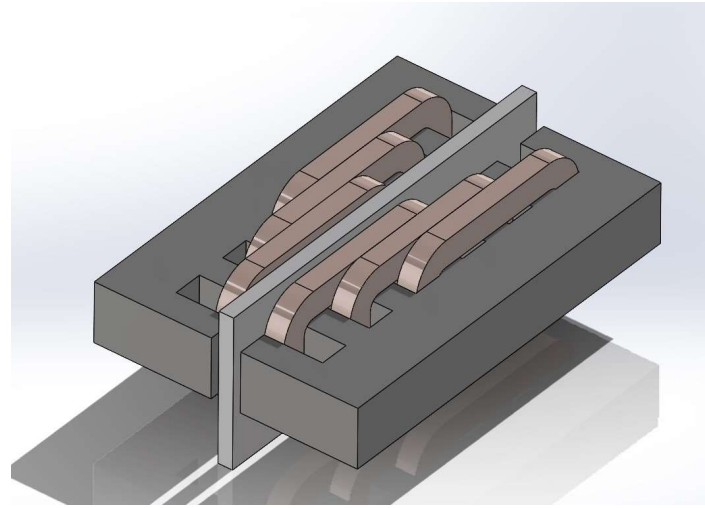


**Figure 4.1: LIM SolidWorks Modeling**

## 4.2 Data Collection Setup

Our Mechanical Engineering project group build a Linear Induction Motor. Our goal is to prove the performance of the motor will improve using T-shape Rail. We first measure the Characteristics of the motor using a normal Vertical Rail, then we switch the rail to T-Shape and see if the performance will improve. In this thesis, we are using 4 different connections to see the performance of the motor. Figure 4.2 shows the physical setup of the testing.



**Figure 4.2: Physical Setup of the Testing**

We set up the circuit with a 3-phase AC source connected to a Power Analyzer then connect to the LIM's coils. The power analyzer will give us current, voltage, and Power. We will be testing 4 different connections of coils, which will be discussed in Section 4.4, Coils connection.

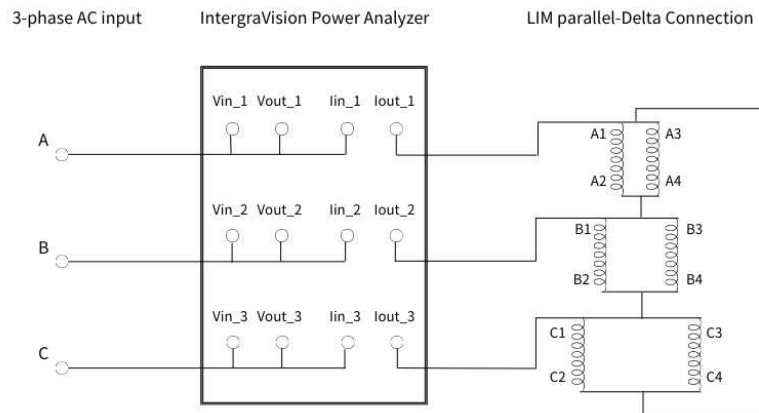


**Figure 4.3: Example: Parallel Delta connection**

Figure 4.3 shows the block diagram of the testing circuit.

### **4.3      Rails selection**

The design of the T-shape rail and vertical rail can have a significant impact on the performance of a linear induction motor. The choice of material and geometry, the magnetic flux density in the air gap between the rails, the distance between the rails, proper alignment, and cooling mechanisms are all critical factors that can affect the efficiency and power output of the motor. An uneven distribution of magnetic flux or improper alignment can result in reduced performance and efficiency while incorporating cooling channels or other cooling mechanisms in the rails can improve the thermal performance of the motor and increase its power output. We are using aluminum for both the T-shape rail and vertical rail to see which one will have better performance.



**Figure 4.4: T-Shape Rail vs Vertical Rail**

### **4.4      Coils Connection**

The Motor we have has six coils, and by connecting them in different ways, we will have different circuits and therefore different outputs. With different connections, we can

see the impact T- shape Rail do on each circuits. Figure 4.5 shows the coils with labels for the LIM we want to test.

We are testing four types of connections: Parallel-Delta, Parallel-Wye, SeriesDelta, and Series-Wye. Each of the circuit diagrams will be shown in the section below. The choice of connection affects the magnetic field generated by the motor and therefore its performance. By testing each one of the connection, we can see which one have better performance.



**Figure 4.5: LIM Coils**

#### 4.4.1      **Parallel-Delta connection**

In a parallel-delta connection, each coil is connected in parallel to the same phase of the AC source at one end, and in a delta (triangular) configuration at the other end. This connection results in a balanced voltage across each coil, but the current through each coil is different. The current through each coil is inversely proportional to its impedance.

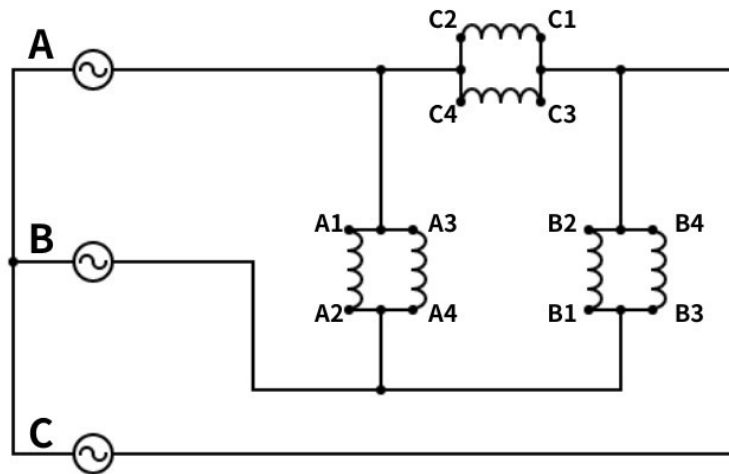


**Figure 4.6: Parallel-Delta connection**

#### 4.4.2      Parallel-Y Connection

In a parallel-Y connection, each coil is connected in parallel to the same phase of the AC source at one end, and in a Y (star) configuration at the other end. This connection results in a balanced current across each coil, but the voltage across each coil is different. This connection is used in LIMs that require high current levels and moderate starting thrust.

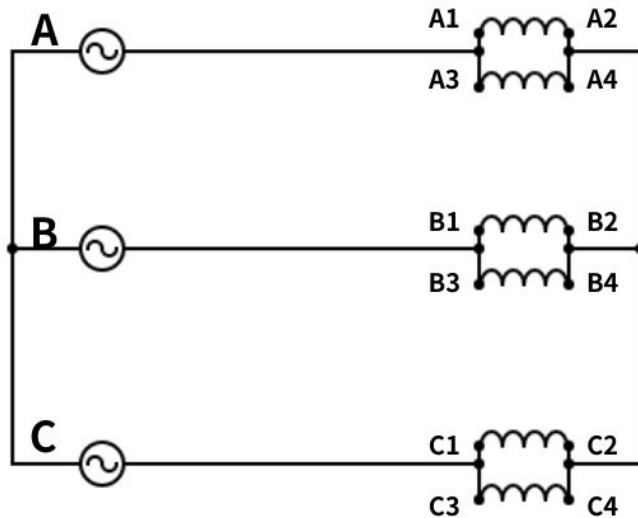


**Figure 4.7: Parallel-Y Connection**

#### 4.4.3 Series-Delta Connection

In a series-delta connection, the coils are connected in series to each other and to the same phase of the AC source. The connection is in a delta configuration at one end and produces a balanced voltage across each coil. The current through each coil is directly proportional to its impedance. This connection is used in LIMs that require high voltage and moderate starting thrust.

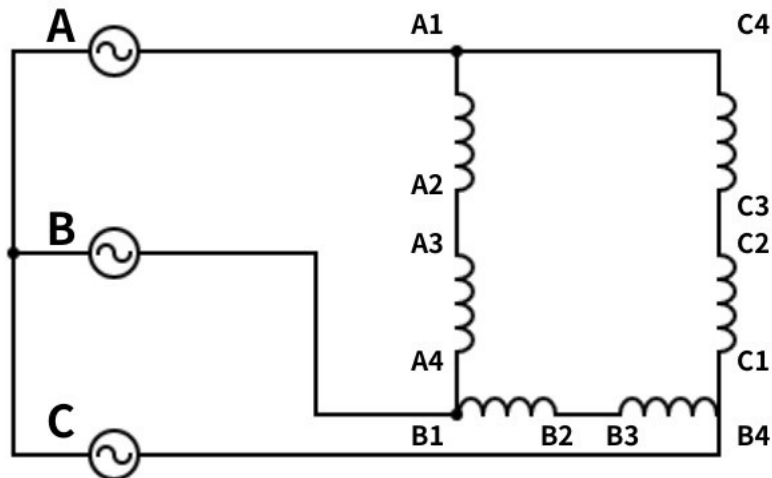


**Figure 4.8: Series-Delta Connection**

#### 4.4.4 Series-Y Connection

In a series-Y connection, the coils are connected in series to each other and to the same phase of the AC source. The connection is in a Y configuration at one end and produces a balanced current across each coil. The voltage across each coil is different.

This connection is used in LIMs that require high voltage and high starting thrust.

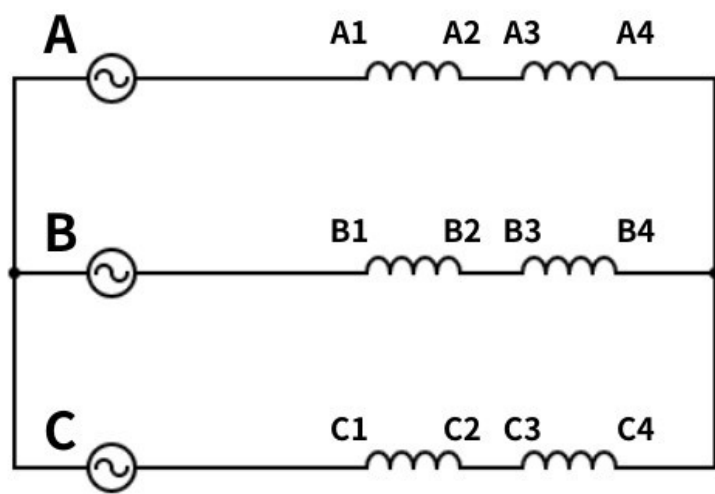


Figure 4.9: Series-Y Connection

# **Chapter 5**

## **TESTING RESULT**

The testing results for the four different connections of coils in a LIM are presented and analyzed in this section.

The raw data collected during the testing process is presented in the form of graphs, which show the voltage and current RMS, active and reactive power, power factor, and pulling force of each connection type as a function of time. The data were measured using a power meter.

### **5.1 Parallel-Delta connection**

For Parallel-Delta connection results showed that both the Vertical Rail and T-Shape Rail configurations had similar pulling force and efficiency, just like Parallel-Y. The pulling force improves by 4.55 % in Parallel-Delta.

#### **5.1.1 Vertical Rail**

Figure 5.1 shows the data collection of the power analyzer and Table 5.1 shows the data collection of the Parallel-Delta with Vertical Rail.

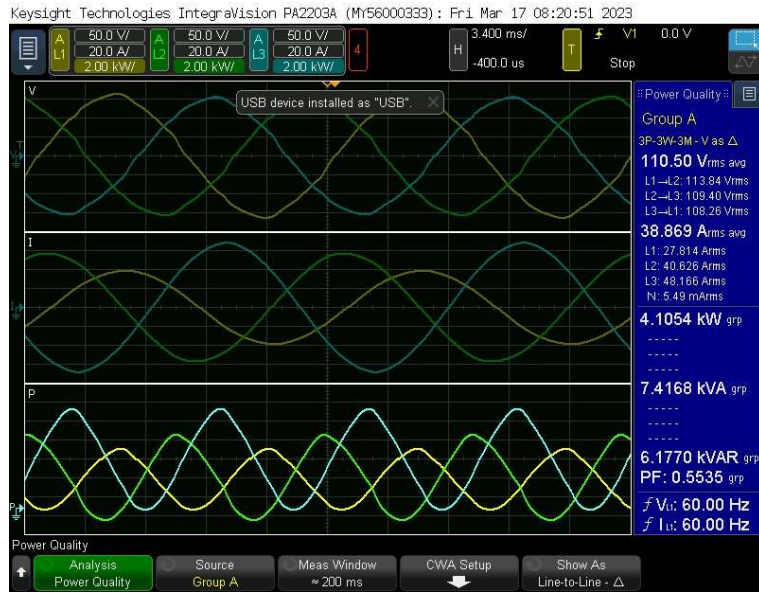


**Figure 5.1: Parallel-Delta with Vertical Rail- 120V Input**

True Voltage Average	A $\Rightarrow$ N Voltage	B $\Rightarrow$ N Voltage	C $\Rightarrow$ N Voltage
110.5 Vrms	113.84 Vrms	109.4 Vrms	108.26 Vrms
3Phase Current Average	A Line Current	B Line Current	C Line Current
38.869 Arms	27.814 A	40.626 A	48.166 A
Active Power	Apparent Power	Reactive Power	Power Factor
4105 W	7417 VA	6177 VAR	0.553
Frequency	Pulling Force		
60 Hz	36.698 N		

**Table 5.1: Parallel-Delta with Vertical Rail- 120V Input data collection**

### 5.1.2 T-Shape Rail

Table 5.2 shows the data collection of the Parallel-Delta with Vertical Rail.

True Voltage Average	A $\Rightarrow$ N Voltage	B $\Rightarrow$ N Voltage	C $\Rightarrow$ N Voltage
110.34 Vrms	113.31 Vrms	109.59 Vrms	108.12 Vrms
3Phase Current Average	A Line Current	B Line Current	C Line Current
39.07 Arms	27.968 A	40.759 A	48.492 A
Active Power	Apparent Power	Reactive Power	Power Factor
4174.3 W	7449.9 VA	6170.6 VAR	0.560
Frequency	Pulling Force		
59.97 Hz	38.366 N		

**Table 5.2: Parallel-Delta with T-Shape Rail- 120V Input data collection**

## 5.2 Parallel-Y Connection

In the Parallel-Y connection, the results showed that both the Vertical Rail and T-Shape Rail configurations had similar pulling force and efficiency. The pulling force improvement is only 3.45 %. Therefore, the use of a T-Shape Rail can slightly improve the power. We can see the Line to Natural Voltage and the power output are not balanced.

### 5.2.1 Vertical Rail

Figure 5.2 shows the data collection of the power analyzer and Table 5.3 shows the data collection of the Parallel-Y with Vertical Rail.

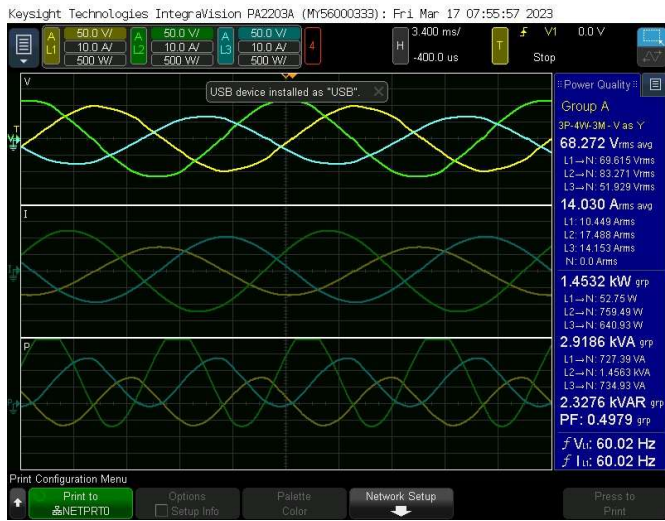


**Figure 5.2: Parallel-Y with Vertical Rail 120V Input**

True Voltage Average	A $\Rightarrow$ N Voltage	B $\Rightarrow$ N Voltage	C $\Rightarrow$ N Voltage
68.466 Vrms	69.865 Vrms	83.948 Vrms	51.555 Vrms
3Phase Current Average	A Line Current	B Line Current	C Line Current
14.001 Arms	10.43 A	17.442 A	14.132 A
Total Active Power	A $\Rightarrow$ N Active Power	B $\Rightarrow$ N Active Power	C $\Rightarrow$ N Active Power
1446.7 W	45.29 W	764.56 W	636.84 W
Total Apparent Power	A $\Rightarrow$ N Apparent Power	B $\Rightarrow$ N Apparent Power	C $\Rightarrow$ N Apparent Power
2921.8 VA	728.98 VA	1464.2 VA	728.59 VA
Reactive Power	Power Factor	Frequency	Pulling Force
2330.3 VAR	0.495	60 Hz	16.125 N

**Table 5.3: Parallel-Y with Vertical Rail 120V Input data collection**

### 5.2.2 T-Shape Rail

Table 5.4 shows the data collection of the Parallel-Y with T-shape Rail.

True Voltage Average	A $\Rightarrow$ N Voltage	B $\Rightarrow$ N Voltage	C $\Rightarrow$ N Voltage
68.505 Vrms	69.993 Vrms	83.886 Vrms	51.635 Vrms
3Phase Current Average	A Line Current	B Line Current	C Line Current
14.148 Arms	10.518 A	17.581 A	14.345 A
Total Active Power	A $\Rightarrow$ N Active Power	B $\Rightarrow$ N Active Power	C $\Rightarrow$ N Active Power
1489.3 W	57.52 W	783.2 W	648.54 W
Total Apparent Power	A $\Rightarrow$ N Apparent Power	B $\Rightarrow$ N Apparent Power	C $\Rightarrow$ N Apparent Power
2951.7 VA	736.21 VA	783.2 VA	740.7 VA
Reactive Power	Power Factor	Frequency	Pulling Force
2341.5 VAR	0.505	59.98 Hz	16.68 N

**Table 5.4: Parallel-Y with T-shape Rail 120V Input data collection**

## 5.3 Series-Delta Connection

The Series-Delta connection results showed that the T-Shpae Rail configuration had a higher Pulling force and efficiency compared to the Vertical Rail configuration. The improvement of the pulling force is about 33.3%, which indicates that the T-Shape Rail configuration may be more suitable for LIMs using a Series-Delta connection.

### 5.3.1 Vertical Rail

Figure 5.3 shows the data collection of the power analyzer and Table 5.5 shows the data collection of the Series-Delta with Vertical Rail.

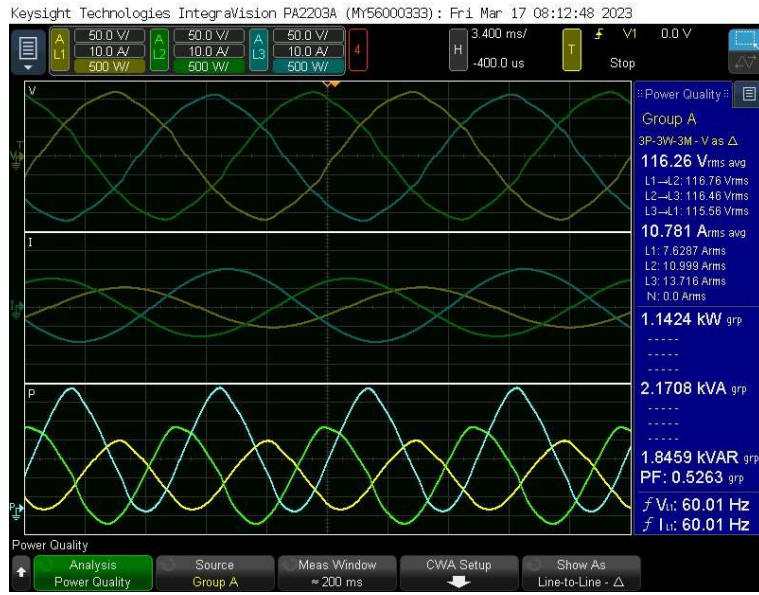


**Figure 5.3: Series-Delta with Vertical Rail 120V Input**

True Voltage Average	A ⇒ B Voltage	B ⇒ C Voltage	C ⇒ A Voltage
116.87 Vrms	117.34 Vrms	117.13 Vrms	116.13 Vrms
3Phase Current Average	A Line Current	B Line Current	C Line Current
10.831 Arms	7.642 A	11.052 A	13.799 A
Active Power	Apparent Power	Reactive Power	Power Factor
1159 W	2192.4 VA	1861 VAR	0.529
Frequency	Pulling Force		
59.98 Hz	5.838 N		

**Table 5.5: Series-Delta with Vertical Rail 120V Input data collection**

### 5.3.2 T-Shape Rail

Table 5.6 shows the data collection of the Series-Delta with T-shape Rail.

True Voltage Average	A $\Rightarrow$ B Voltage	B $\Rightarrow$ C Voltage	C $\Rightarrow$ A Voltage
116.15 Vrms	116.44 Vrms	116.6 Vrms	115.41 Vrms
3Phase Current Average	A Line Current	B Line Current	C Line Current
10.896 Arms	7.725 A	11.063 A	13.9 A
Active Power	Apparent Power	Reactive Power	Power Factor
1172.4 W	2192.6 VA	1852.8 VAR	0.535
Frequency	Pulling Force		
59.98 Hz	7.784 N		

**Table 5.6: Series-Delta with T-Shape Rail- 120V Input data collection**

### 5.4 Series-Y Connection

For the Series-Y connection, Results showed that the T-Shpae Rail configuration had a higher Pulling force and efficiency compared to the Vertical Rail configuration. The improvement of the pulling force is about 150%, which is the best in all the connections we have.

### 5.4.1 Vertical Rail

Figure 5.4 shows the data collection of the power analyzer and Table 5.7 shows the data collection of the Series-Y with Vertical Rail.

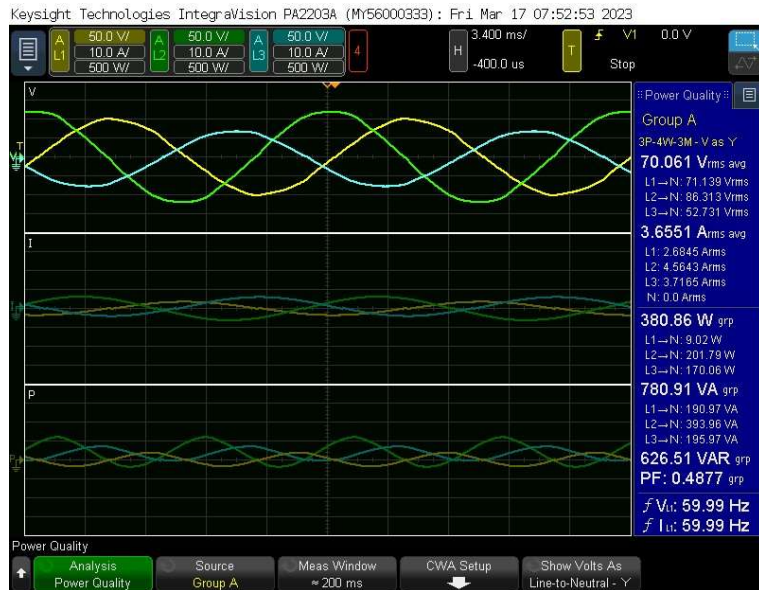


**Figure 5.4: Series-Y with Vertical Rail 120V Input**

True Voltage Average	A ⇒ N Voltage	B ⇒ N Voltage	C ⇒ N Voltage
70.1 Vrms	71.14 Vrms	86.313 Vrms	54.73 Vrms
3Phase Current Average	A Line Current	B Line Current	C Line Current
3.65 Arms	2.68 A	4.56 A	3.72 A
Total Active Power	A ⇒ N Active Power	B ⇒ N Active Power	C ⇒ N Active Power
380.86 W	9.02 W	201.79 W	170.06 W
Total Apparent Power	A ⇒ N Apparent Power	B ⇒ N Apparent Power	C ⇒ N Apparent Power
780.91 VA	190.97 VA	393.96 VA	195.97 VA
Reactive Power	Power Factor	Frequency	Pulling Force
626.51 VAR	0.488	60 Hz	0.556 N

**Table 5.7: Series-Y with Vertical Rail 120V Input data collection**

### 5.4.2 T-Shape Rail

Table 5.8 shows the data collection of the Series-Y with T-Shape Rail.

True Voltage Average 70.2 Vrms	A $\Rightarrow$ N Voltage 71.34 Vrms	B $\Rightarrow$ N Voltage 86.5 Vrms	C $\Rightarrow$ N Voltage 52.75 Vrms
3Phase Current Average 3.71 Arms	A Line Current 2.71 A	B Line Current 4.62 A	C Line Current 3.78 A
Total Active Power 393.7 W	A $\Rightarrow$ N Active Power 11.89 W	B $\Rightarrow$ N Active Power 208.3 W	C $\Rightarrow$ N Active Power 173.5 W
Total Apparent Power 792.94 VA	A $\Rightarrow$ N Apparent Power 193.73 VA	B $\Rightarrow$ N Apparent Power 399.61 VA	C $\Rightarrow$ N Apparent Power 199.59 VA
Reactive Power 632.99 VAR	Power Factor 0.497	Frequency 59.98 Hz	Pulling Force 1.39 N

**Table 5.8: Series-Y with T-Shape Rail 120V Input data collection**

## 5.5 Result Analysis

Type	Pulling Force using Vertical Rail	Pulling Force using T-Shape Rail	Force Improvement
Parallel Y	16.12 N	16.68 N	3.45%
Parallel Delta	36.70 N	38.37 N	4.55%
Series Y	0.56 N	1.39 N	150%
Series Delta	5.84 N	7.78 N	33.33%

**Table 5.9: Force Comparison**

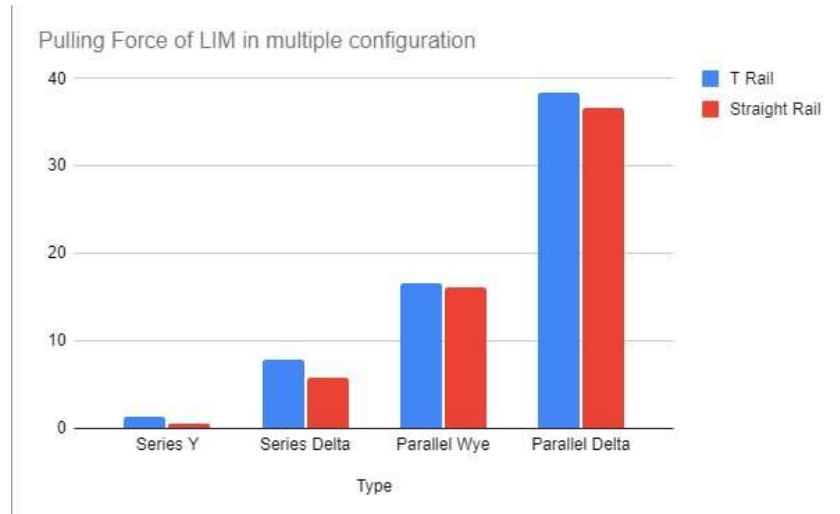


**Figure 5.5: Pulling force comparison**

Based on the results shown in table 5.9, figure 5.6 and, figure 5.5, for the ParallelY and Parallel-Delta connections, it can be concluded that the use of a T-Shape Rail configuration can provide a slight improvement in pulling force and efficiency compared to the Vertical Rail configuration. However, the improvement is relatively small, with a 3.45% increase in pulling force for the Parallel-Y connection and a 4.55% increase for the Parallel-Delta connection.

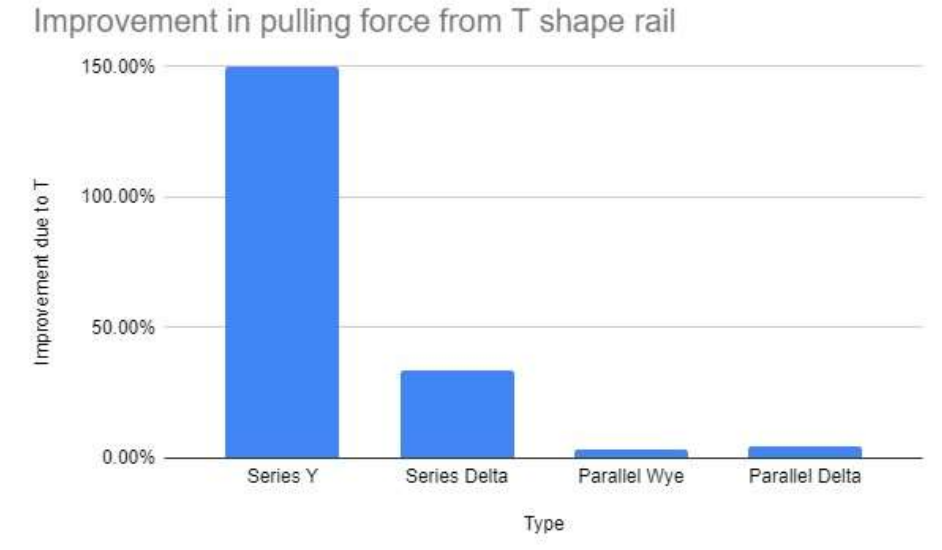


**Figure 5.6: Force Improvement due to T-Shape Rail**

Based on the results for the Series-Delta and Series-Y connections, it can be concluded that the T-Shape Rail configuration is more suitable for LIMs using these types of connections. In both cases, the T-Shape Rail configuration provided a significant improvement in pulling force and efficiency compared to the Vertical Rail configuration.

Specifically, for the Series-Delta connection, the T-Shape Rail configuration provided a 33.3% increase in pulling force, while for the Series-Y connection, the improvement was even more significant, with a 150% increase in pulling force.

In comparison, the improvements observed in the Parallel-Y and Parallel-Delta connections were relatively small, with increases in pulling force of only 3.45% and 4.55%, respectively.

The analysis of the test results revealed an interesting observation regarding the current and power output balance in the LIM. It was consistently observed that the data for current

and power output exhibited an imbalance. However, it is important to note that this imbalance is a characteristic of LIMs and not indicative of any issues with the motor itself.

The physical nature of LIMs inherently leads to an unbalanced distribution of current and power output. This phenomenon arises from the interaction between the magnetic fields, induced currents, and the asymmetry of the motor structure. The uneven distribution of current and power output is a result of the specific design and operation principles of LIMs.

To address this imbalance and improve the performance of the LIM, one possible approach is to increase the number of teeth in the motor structure. By increasing the number of teeth, the magnetic flux distribution can be better controlled, leading to a more balanced current and power output. This adjustment in the motor's physical design can help mitigate the inherent imbalance and potentially improve overall performance.

It is important to acknowledge that achieving a perfect balance in current and power output may not be possible due to the inherent nature of LIMs. However, by understanding and recognizing this characteristic, appropriate design modifications can be implemented to optimize performance and minimize the effects of imbalance.

# Chapter 6

## LIM APPLICATION

### 6.1 Snowmobile

The integration of LIMs in snowmobiles has garnered significant attention as a means to enhance their performance and efficiency on snow-covered terrains. LIMbased snowmobiles offer advantages such as improved traction and acceleration, which contribute to better control and maneuverability in challenging snowy conditions.

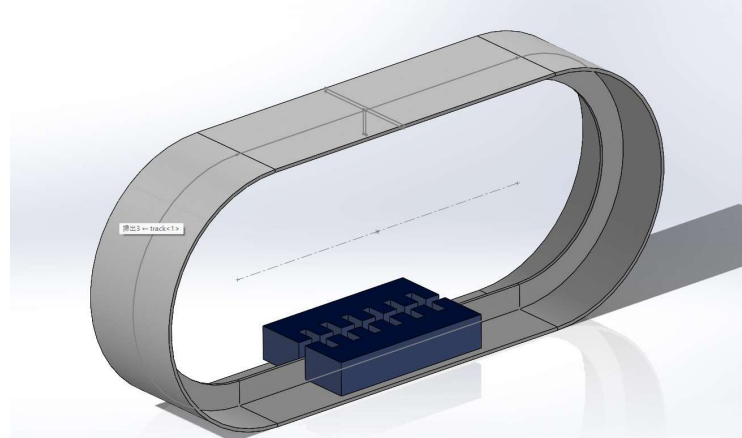


**Figure 6.1: LIM Snowmobile SolidWork**

Literature reviews have demonstrated the feasibility and potential performance enhancement of LIM-based snowmobiles [1]. conducted a comprehensive study on the performance analysis of linear induction motor-based snowmobiles. Their research showcased the improved speed and efficiency achieved through LIM integration compared to traditional internal combustion engine-powered snowmobiles [2]. focused on optimizing

the design of the linear induction motor specifically for snowmobile applications, considering factors such as power requirements, thermal management, and weight distribution.



**Figure 6.2: LIM Snowmobile Design**

These literature reviews underscore the potential benefits of utilizing LIM technology in snowmobiles, particularly in terms of traction, acceleration, and overall performance [8].

## 6.2 E-Bike

The electric bike, or e-bike, has emerged as a popular alternative to traditional bicycles, offering eco-friendly transportation with assisted pedaling. Integrating linear induction motors (LIMs) in e-bikes provides several advantages, including enhanced power delivery, improved performance, and extended range.

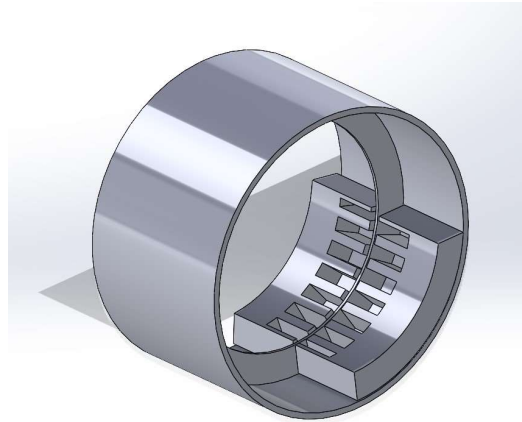


**Figure 6.3: LIM E-Bike Application**

Literature reviews have indicated a growing interest in the integration of LIM technology in e-bikes [3]. focused on optimizing the design of the linear induction motor specifically for e-bike applications. Their study considered factors such as power requirements, weight reduction, and thermal management to achieve an optimal design [4]. explored the integration of LIM technology with advanced control algorithms to further improve the efficiency and performance of e-bikes[7].

These literature reviews highlight the potential benefits of utilizing LIM technology in e-bikes, such as improved power delivery, increased range, and enhanced efficiency.

### **6.3     Elevator**

Elevators play a crucial role in vertical transportation systems, offering convenient access to various levels of buildings and structures. The integration of linear induction motors (LIMs) in elevator systems has gained attention due to the advantages they offer,

including smooth and efficient operation, reduced maintenance requirements, and improved energy efficiency.

U.S. Patent Dec. 29, 1992 Sheet 1 of 4 5,174,416

FIG. I

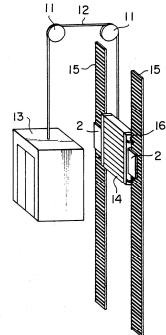


**Figure 6.4: LIM elevator Application**

Extensive research has been conducted on the use of LIMs in elevator applications [5]. investigated the dynamic performance and control strategies of LIM-based elevator systems, considering factors such as speed control, position accuracy, and vibration reduction[6]. focused on optimizing the design of the linear induction motor specifically for elevator applications, taking into account power requirements, efficiency, and noise reduction.

These literature reviews emphasize the potential advantages of utilizing LIM technology in elevator systems, including enhanced reliability, reduced maintenance costs, and improved energy efficiency.

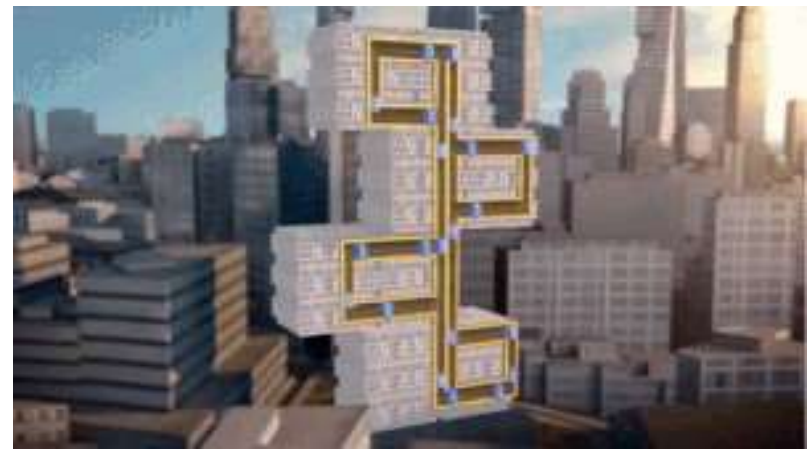


**Figure 6.5: LIM elevator Application 2nd**

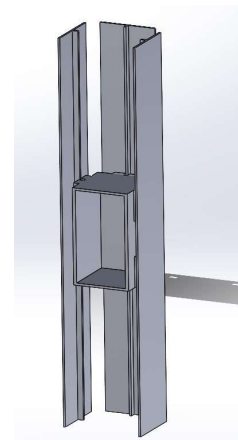


**Figure 6.6: LIM elevator SolidWork**

# **Chapter 7**

## **FUTURE WORK**

### **7.1 Size and Geometry**

Further investigation is needed to optimize the size and geometry of LIMs for specific applications. This involves considering factors such as space limitations, weight, and efficiency. Exploring advanced manufacturing techniques and materials can help achieve more compact and lightweight LIM designs without compromising performance.

### **7.2 Material Selection**

Future research can focus on developing materials with enhanced magnetic properties, improved thermal conductivity, and higher mechanical strength. This can contribute to better LIM performance and durability. Additionally, investigating sustainable and eco-friendly materials aligns with the growing demand for environmentally conscious technologies.

### **7.3 Coil Connection Design**

Innovative coil connection designs can be explored to improve LIM efficiency, power output, and torque characteristics. This includes investigating advanced winding techniques and configurations to enhance magnetic field distribution and reduce power losses.

## **7.4 Rail Selection**

Research can compare different rail materials and designs to optimize LIM performance and reduce energy losses. Innovative rail shapes and surface coatings can also be investigated to minimize friction, wear, and noise, thereby improving overall efficiency and reliability.

## **7.5 Power Electronics**

Advancements in power electronic systems, such as motor controllers and converters, can enhance the control and efficiency of LIMs. Developing smart grid and energy management technologies can optimize LIM performance in terms of power consumption and grid interaction.

## **7.6 Testing**

Continued experimental testing and validation of LIMs under various operating conditions are crucial. This includes different loads, speeds, and environmental factors. Developing standardized testing procedures and performance metrics can facilitate accurate and consistent performance evaluation and comparison.

## **7.7 Safety**

Further research is needed to implement safety features and mechanisms in LIM designs to ensure reliable operation and protection against electrical hazards. Compliance with international safety standards and regulations should be considered, along with the exploration of additional safety measures specific to LIMs.

These future research directions aim to advance the field of Linear Induction Motors, optimize their performance, and contribute to their wider adoption in various applications. By addressing the challenges and exploring these areas, LIMs can further enhance their efficiency, reliability, and suitability for emerging technological needs.

# **Chapter 8**

## **Conclusion**

In conclusion, this thesis has focused on the study and analysis of Linear Induction Motors (LIMs) with the aim of understanding their unique characteristics, improving their performance, and exploring potential applications.

Through a comprehensive examination of LIM fundamentals, including the principles of operation and physical aspects, we have gained a deeper understanding of the technology.

Experimental investigations were conducted on a laboratory-scale LIM, considering different coil connections and rail designs. The results revealed that the parallel-delta coil connection exhibited superior performance in terms of pulling force and power output, while the use of a T-shape rail demonstrated improvements across various coil connections, particularly in the series-Y and series-delta configurations.

These findings indicate the potential for optimizing LIM performance through careful consideration of coil connections and rail designs. The parallel-delta connection and T-shape rail configuration show promise for enhancing LIM efficiency and power.

Furthermore, this thesis has presented three potential future applications of LIM technology, including snowmobile, e-bike, and elevator systems. By showcasing simplified 3D models, we have provided insights into how LIMs can be integrated into these applications, leveraging their advantages for improved performance and energy efficiency.

In summary, this thesis has contributed to the understanding of LIM technology, identified optimal coil connections and rail designs, and explored potential applications.

The findings and insights gained from this research can serve as a foundation for further advancements in LIM technology, leading to enhanced performance, efficiency, and sustainability in various industrial and transportation sectors.

# BIBLIOGRAPHY

- [1] S. Yamamura,. *Theory of Linear Induction Motors*, 1st ed.. Wiley, 1972.
- [2] M. Larsson. *Electric Motors for Vehicle Propulsion*. Linköpings Universitet, 2014.
- [3] S. Chevallie. *Comparative Study and Selection Criteria of Linear Motors*, Ecole Polytechnique Fédérale de Lausanne. Lausanne, 2006.
- [4] J. Smajic. *Theory of Linear Induction Motor (LIM)*. Zurich, 2018.
- [5] J. Pyrhönen, T. Jokinen and V. Hrabovcova'. *Design of Rotating Electrical Machines*. John Wiley and Sons, 2008.
- [6] S. Sakab. "Linear induction motor for elevators". Mitsubishi Electric Corp, 1992.
- [7] E. R. Laithwaite. *Propulsion without Wheels*. English Universities Press, 1970.
- [8] W. Hayt and J. Buck,. *Engineering Electromagnetics*. New York: McGraw-Hill, 2012.
- [9] J. -H. Jeong, J. Lim, C. -W. Ha, C. -H. Kim and J. -Y. Choi. *Thrust and efficiency analysis of linear induction motors for semi-high-speed Maglev trains using 2D finite element models*. Korea, 2016.
- [10] M. Jufer and A. Cassa. *Collaboration with the Korean Railroad*. Jstor, 2010.
- [11] S. K. *What is a Linear Induction Motor “LIM”? Working Principle and Applications*. electricaltechnology, 2018.
- [12] E. R. Laithwaite. "Linear Induction Motor for Vehicle Propulsion". England Patent, 1971.